Examination of time-reversal acoustics in shallow water and applications to noncoherent underwater communications

Kevin B. Smith,[a] Antonio A. M. Abrantes, and Andres Larraza
Department of Physics, Naval Postgraduate School, Monterey, California 93943

(Received 1 October 1999; revised 12 September 2002; accepted 27 February 2003)

The shallow water acoustic communication channel is characterized by strong signal degradation caused by multipath propagation and high spatial and temporal variability of the channel conditions. At the receiver, multipath propagation causes intersymbol interference and is considered the most important of the channel distortions. This paper examines the application of time-reversal acoustic (TRA) arrays, i.e., phase-conjugated arrays (PCAs), that generate a spatio-temporal focus of acoustic energy at the receiver location, eliminating distortions introduced by channel propagation. This technique is self-adaptive and automatically compensates for environmental effects and array imperfections without the need to explicitly characterize the environment. An attempt is made to characterize the influences of a PCA design on its focusing properties with particular attention given to applications in noncoherent underwater acoustic communication systems. Due to the PCA spatial diversity focusing properties, PC arrays may have an important role in an acoustic local area network. Each array is able to simultaneously transmit different messages that will focus only at the destination receiver node. [DOI: 10.1121/1.1570831]

PACS numbers: 43.30.Bp [SAC-B]

I. INTRODUCTION

Traditionally, applications for underwater acoustic (UWA) communication systems were almost exclusively military. In the last 10 years there has been a growing need for UWA communication systems for commercial applications. As a consequence, an increase in research and development of UWA communication systems has occurred. Applications that have received much attention lately are secure military communications, pollution monitoring, and remote control in off-shore oil industry and video telemetry, to name a few. Many of the applications being developed are now calling for near real-time communication with submarines and remotely operated vehicles. As the UWA communications channel has limited bandwidth available, the bandwidth efficiency becomes an important issue for a UWA communication system. There have been several excellent reviews of recent advances in underwater communications and telemetry presented by Baggeroer (1984), Catipovic (1990), Coates *et al.* (1993), and Stojanovic (1996).

The shallow water acoustic communication channel is characterized by strong signal degradation caused by multipath propagation and high spatial and temporal variability of the channel conditions. In any underwater acoustic environment there is limited bandwidth available due to transmission loss which increases with both frequency and range. This is a major constraint in underwater communication systems design. The most important of the difficulties encountered in shallow water acoustics digital communications is considered to be the time-varying multipath propagation. This leads to a requirement for powerful and reliable receiver algorithms for signal processing in shallow water environments. In recent years there has been a large effort made in the design of techniques and algorithms to overcome this problem.

In a digital communication system, multipath propagation causes intersymbol interference (ISI). As an example, in a medium-range, 6-km-long, shallow water (200 m) channel, a typical value for multipath delay spread is 30 ms. If the communication system is signaling at 1 kilosymbol per second, the ISI will extend over 30 symbols, making it difficult for a receiver to recover the original message.

In shallow water regions, multipath is primarily due to reflections at the surface and bottom of the channel but can also be caused by refracted paths under certain environmental conditions. The multipath structure depends on the channel geometry, sound speed structure, frequency of transmitted signals, and on the source and receiver locations. On a small time scale, the most important contribution to channel variability is surface scattering due to waves producing time-varying multipaths. On a larger time scale, channel variations are due to a variety of effects including internal waves, temperature gradients, and currents in the sound speed profile. The temporal variability is also frequency dependent.

The ISI and strong phase fluctuations caused by multipath propagation and temporal channel variability have in the past led to system designs based exclusively on noncoherent detection methods. These systems have poor spectral efficiency and low signaling rates and are still in use when robustness is the principal requirement in system design. To treat the ISI problem, these systems insert delay times between consecutive pulses to ensure that all the reverberation and multipath structure will vanish before each subsequent pulse is received (Stojanovic, 1996). This can significantly reduce the available data throughput.

In recent years, the feasibility of bandwidth-efficient phase-coherent modulation techniques for UWA communications has been proven (Stojanovic *et al.*, 1993, 1994, 1995).

[a]Electronic mail: kbsmith@nps.navy.mil

Several systems have been proposed and implemented using differential and purely coherent detection methods, thereby increasing the data throughput. However, these systems must still treat ISI in the received signal and be able to track any phase variations due to changing channel conditions. Typically these systems employ either some form of array processing, for exploitation of spatial diversity, or equalization or a combination of both.

Array processing at both the source and receiver end have been used for multipath suppression. Coates (1993) and Galvin and Coates (1994) describe an approach that uses transmitter arrays to excite only a single path of propagation. However, long arrays are required and small errors in positioning can degrade performance. In general, this technique was found to be more effective at shorter ranges.

Another approach (Howe *et al.*, 1994; Tarbit *et al.*, 1994; Henderson *et al.*, 1994) is based on adaptive beamforming at the receiver end. It uses a least mean squares (LMS) type of algorithm to adaptively steer nulls in the direction of the surface reflected wave. Naturally, as the multipath structure increases in range, it was found to decrease in performance as the range increases in relation to depth (Tarbit *et al.*, 1994). In order to enhance the performance of the beamformer, an equalizer was proposed by Howe *et al.* (1994) of a decision-feedback type. This system operates under a LMS algorithm with low computational requirements, allowing real-time adaptation at the symbol rate.

A different approach based on purely phase-coherent detection methods is described by Stojanovic *et al.* (1993, 1994, 1995). These methods attempt to counter the effect of phase variations and ISI by combining joint synchronization and equalization. It incorporates spatial signal processing based on combining diversity and a fractionally spaced decision-feedback equalization with a recursive least squares (RLS) algorithm.

From the previous examples of communication systems, it is obvious that complex systems and high computational requirements are needed to handle channel distortion and ISI encountered in the underwater acoustic channel. Such systems can exceed the speeds of available hardware. At high symbol rates, the long ISI requires large adaptive filters, therefore increasing the computational complexity.

The aim of the present paper is to provide an original and relatively simple algorithm to overcome the ISI problem in a shallow water channel. This solution is not based on sophisticated processing algorithms but is equivalent to matched field processing with the filter matched to the impulse response of the ocean. The low computational load required in this technique is due to the fact that it uses the ocean itself as the matched filter for the acoustic propagation between source and receiver. By using rather simple signal processing at the transmitter (suitable for real-time implementation) the multipath structure at the receiver end is virtually absent, allowing a reduced-complexity receiver structure.

This technique uses time-reversal acoustic (TRA) arrays to generate a spatio-temporal focus of acoustic energy at the receiver location, eliminating (or greatly reducing) distortions introduced by channel propagation. The application of TRA to the underwater communications problem has previously been suggested by Jackson and Dowling (1992) and Kuperman *et al.* (1998). The first known application of TRA which developed a signaling scheme for communication purposes was introduced by Abrantes *et al.* (1999). This paper provides the details of much of that work.

The analysis presented here is based purely on numerical modeling results. The numerical model used throughout is the Monterey–Miami Parabolic Equation (MMPE) acoustic propagation model (Smith, 2001), an upgraded version of the University of Miami Parabolic Equation (UMPE) model (Smith and Tappert, 1994). Both versions are available freely on the web at http://oalib.njit.edu/pe.html.

It should be noted that experimental work has been performed which confirms the usefulness of this approach (Heinemann, 2000). The results from that work are presented in a companion article. Additional numerical and experimental work are on-going in the development of more sophisticated signaling techniques.

The remainder of this paper is organized as follows. Section II presents a brief overview of time-reversal acoustics theory. In particular it analyzes the case of time-reversal acoustics in a range-independent channel and a more general static range-dependent channel. In these ideal situations, closed-form solutions for the field at the focus have previously been developed, and some focusing properties can be inferred and may be extrapolated for more general environments. In Sec. III the focusing properties of the time-reversal array are studied through MMPE numerical simulations. It shows how the time-reversal array focusing properties change when the array operates at different carrier frequencies, and when the array length or the array element spacing is altered. Also presented are the frequency characterization of the channel and examples of how range shifting of the focus location can be attained. Section IV describes applications of time-reversal arrays to UWA communications and Sec. V presents a summary of conclusions and identifies some aspects of TRA communications modeling requiring further research.

II. THEORETICAL BACKGROUND AND NUMERICAL EXAMINATIONS

Much of the theoretical development on the phenomenon of time-reversal acoustics has been presented by Jackson and Dowling (1991, 1992), Kuperman *et al.* (1998), and Song *et al.* (1998). The reader is referred to those papers for a more thorough treatment of TRA theory. Each of these previous papers has presented numerical simulations examining various features of the time-reversed field at the position of the focus, including the design of the array. In this section, we shall present specific examples of the focusing properties for our simulated environment and the effects of various array geometries and the implications for communications.

For simplicity, consider a waveguide with pressure-release surface and rigid bottom as depicted in Fig. 1 where the axis from o' to o will be the reference axis for propagation from the receiver array to the source. From the axis location in Fig. 1 the coordinates are related by $z' = z$ and

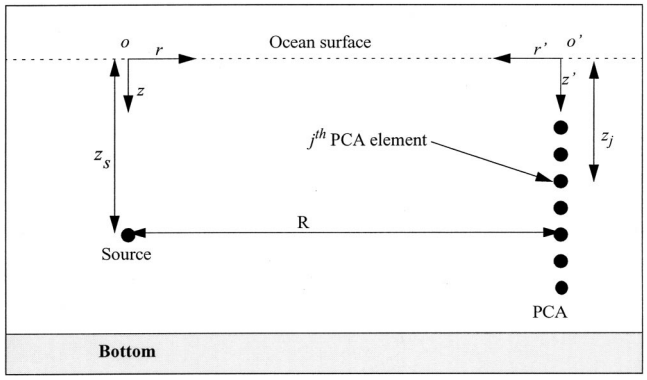

FIG. 1. Waveguide geometry.

$r'=R-r$. In this environment the frequency-domain wave equation, or Helmholtz equation, for a range-independent waveguide can be written as (e.g., Jensen *et al.*, 1994)

$$[\nabla^2+k^2(z)]G(r,z|z_s,\omega)=-\delta(r)\,\delta(z-z_s), \tag{1}$$

where $k(z)=\omega/c(z)$ is the acoustic wavenumber for a waveguide with sound speed $c(z)$, ω denotes the angular frequency, and $G(r,z|z_s,\omega)$ is the frequency-dependent Green's function in cylindrical coordinates at location (r,z) due to a point source located at range $r=0$ and depth $z=z_s$. Note that the depth z is taken positive downward.

From a linear systems theory point of view, the Green's function $G(r,z|z_s,\omega)$ represents the ocean impulse response between a point source located at range $r=0$ and depth $z=z_s$ and a point receiver at location (r,z). It can easily be shown (e.g., Jensen *et al.*, 1994) that $G(r,z|z_s,\omega)$ satisfies the principle of reciprocity,

$$\rho(\vec{r}_s)G(\vec{r}_j|\vec{r}_s,\omega)=\rho(\vec{r}_j)G(\vec{r}_s|\vec{r}_j,\omega), \tag{2}$$

where $\vec{r}_s$ represents the position of a point source and $\vec{r}_j$ indicates the position of a point receiver, i.e., the jth element of the array. Since the density is nearly constant throughout the ocean, this leads to reciprocity of the acoustic field itself. The reciprocity theorem plays a fundamental role in time-reversal acoustics because it implies that the field from an array element propagates to the source location in a reciprocal way as the field from the source to the array element. It is important to note, however, that "time-reversal" only applies to the manipulation of the signal at the time-reversal array elements, and does not imply a reversibility of the propagation itself. This differentiates reciprocity from reversibility. Hence, higher losses incurred along some paths more than others will not be undone via a time-reversal approach.

If a source at position $r=0$, $z=z_s$ transmits a pulse $s(t)$, the jth element of the PCA a distance $r=R$ away records the time-domain signal $p(R,z_j,t)$. The total field back at the original source location, $(r'=0,z_s)$, is given by the superposition of the field produced by each individual array element, which in the time-domain is given by (Kuperman *et al.*, 1998)

$$p_{\mathrm{TRA}}(0,z_s,t)=\frac{1}{(2\pi)^2}\int\left(\sum_{j=1}^{J}\left[\int g_{t'+t''}(R,z_j|z_s,\omega)\times g_{t'}(R,z_s|z_j,\omega)\,dt'\right]s(t''-t+T)\right)dt'', \tag{3}$$

where $g_{t'+t''}(R,z_j|z_s)$ and $g_{t'}(R,z_s|z_j)$ are the time-domain representations of the Green's function. Note that in a time-invariant environment, reciprocity states that these are identical.

The following observations have been made about Eq. (3) (Kuperman *et al.*, 1998):

(i) The integral over t' defines the autocorrelation of the Green's function between the source and the jth element of the PCA. This operation is equivalent to a matched-filter which compresses the time elongation due to multipaths, forming a temporal focus.
(ii) The sum over the array elements is a form of spatial matched filtering, forming a spatial focus.
(iii) The sidelobes of the matched filters for each array element tend to cancel with the sum over the array elements. This is also analogous to broadband matched-field processing results (Brienzo and Hodgkiss, 1993) which further improves temporal focusing.
(iv) The integral over t'' is a convolution of each matched-filtered response with the delayed and time-reversed transmitted pulse. Thus, a slightly degraded and time-reversed version of the original signal is received.

Although the numerical solutions presented in this paper are generated by a parabolic equation model, it is useful in the discussion to consider the field in the context of normal modes. The solutions are then defined in terms of depth-dependent eigenfunctions, or normal modes, and range-dependent Hankel functions. In the frequency domain, Kuperman *et al.* (1998) have shown that a modal decomposition of the time-reversed field in a range-independent environment is given by

$$P_{\mathrm{TRA}}(0,z_s,\omega)\cong\frac{S^*(\omega)e^{i\omega T}}{8\pi RK}\sum_m\frac{\Psi_m(z)\Psi_m(z_s)}{\rho(z_s)}=\frac{S^*(\omega)e^{i\omega T}}{8\pi RK}\,\delta(z-z_s), \tag{4}$$

where $S(\omega)$ is the Fourier representation of the initial transmitted signal $s(t)$, $\Psi_m(z)$ are the depth-separated normal modes of the waveguide, K is a typical horizontal wavenumber component of the propagating modes, $\rho(z_s)$ is the density at the original source location, and $\delta(z-z_s)$ is the Dirac delta function centered at the source location.

This equation shows the vertical focusing performed by the PCA at the range of the original source location due to the closure property of the modes. If the array has only a few elements and cannot properly sample the propagating modes, one can conclude that this focusing will be degraded. As will

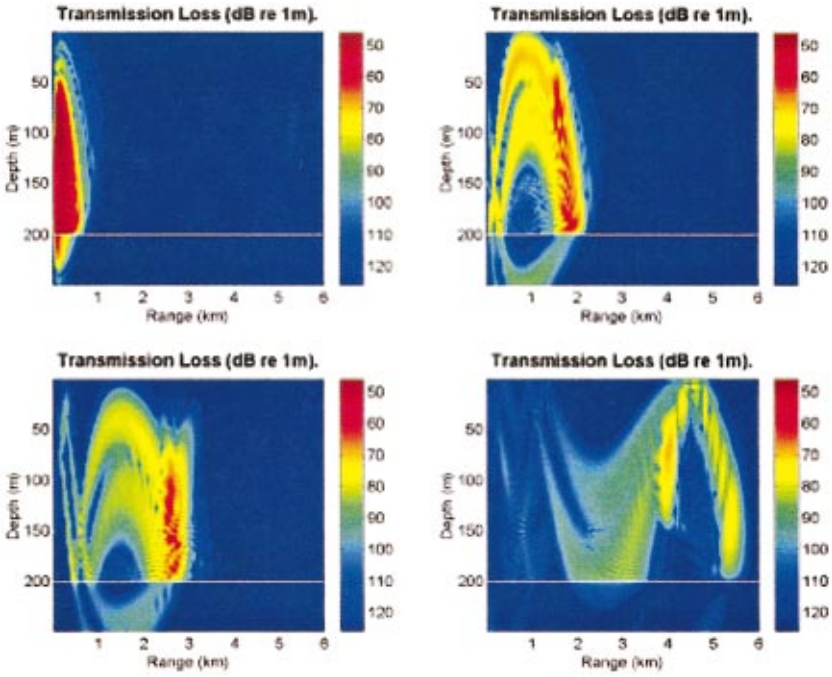

FIG. 2. Single pulse propagation in a shallow water channel.

be confirmed in this paper, numerical simulations indicate that even with a small array aperture, a good quality of temporal focus can still be achieved.

If the environment were range dependent, Kuperman *et al.* (1998) have shown that the time-reversed pressure field satisfies a similar expression. Furthermore, they point out that the focus is independent of the exact nature of the range-independent environment between the source and the PCA. The focus depends only on the local properties of the water column and the sea floor. Therefore, this suggests that, neglecting absorption losses and cylindrical spreading, the focus pattern is independent of the distance between the source and the array. Thus all the general features of a communication scheme based on time-reversal acoustics discussed in this paper should also exist in more general, range-dependent environments.

One should bear in mind, however, that losses due to absorption and scattering are expected to cause attenuation of higher-order modes. As a consequence, the focus is expected to become more blurry than that in the previous ideal lossless situation. Furthermore, as the distance between the array and the focus increases, the focus becomes blurrier due to the strong range and mode number dependence of attenuation. Such influences will not be specifically treated in this analysis.

Figures 2–4 present numerical modeling results of acoustic pulse propagation from the source to the time-reversal array (forward propagation) and the propagation from the time-reversal array to the source (backward propagation). Figure 2 illustrates single pulse propagation from a source located 150 m deep at the origin to a vertical array 6 km away. This pulse has a carrier frequency of 800 Hz and its spectrum spans over 100 Hz with a -3 dB bandwidth of 36.6 Hz. The complete description of this range-independent channel can be found in Sec. III. Figure 3 illustrates the transmitted signal and the multipath arrival structure of the recorded signal by the 150-m-deep array element. Figure 4 represents four snap-shots of the wavefield propagation from the PCA to the source. The spatial focusing at the source location is clearly observable in the lower left panel. Due to the time-reversal transformation at the PCA, the received signal has the time-reversed signature of the signal which was transmitted originally. Similar simulations examining the spatial structure of the focus region have previously been performed by Kuperman *et al.* (1998) and Song *et al.* (1998).

As stated earlier, this phase-conjugation process takes advantage of spatial reciprocity which is a property of wave propagation in a medium with stable refractive index. In general, reciprocity requires a static environment. TRA focusing requires spatial reciprocity in order to construct the exact

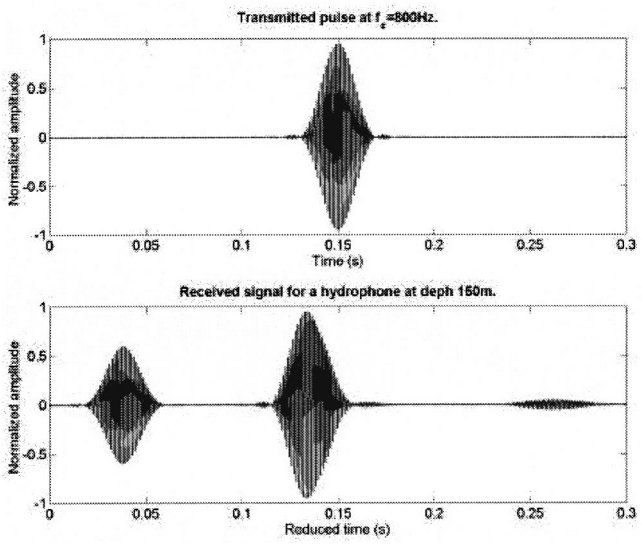

FIG. 3. Transmitted signal from point source 150 m deep (upper panel) and received signal on a single array element at range 6 km and depth 150 m (lower panel).

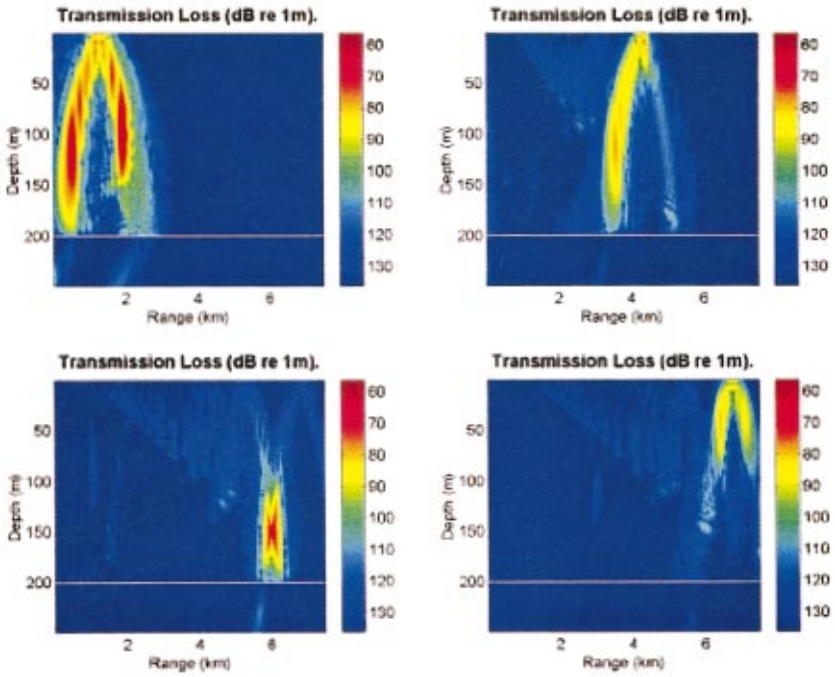

FIG. 4. Time-reversed propagation from the PCA. Note focus appears at original source location, range 6 km, depth 150 m.

time-reversed wavefield that will focus at the original source location. In this way, all the PCA elements transmit back to the source in a reciprocal fashion, and the time-reversed wavefield will have the multipath structure undone at the source location.

Since the PCA only ''learns'' the medium structure that is imprinted in the incoming signal at the instant of its reception, it cannot compensate for refractive fluctuations that occur after reception of the signal, decreasing the focusing properties of the PCA. Also, if the environment or its boundaries change (due to surface waves, internal waves, temperature gradients, receiver or PCA motion, etc.), reciprocity is violated and the focusing properties of the PCA are degraded. To accommodate for temporal changes in the channel, the PCA may need to update the transfer function of the environment with some periodicity that depends on how fast environmental changes affect the focusing properties. Such dynamic interactions would have to be considered in the development of any general communications link.

III. ENVIRONMENTAL INFLUENCES IN TIME-REVERSAL ACOUSTICS

The purpose of the analysis presented here is to examine the features of the focus in the context of a communications algorithm and the influence of variations in the signal and PCA. During the TRA examination process that led to this paper, several other environments were considered. In all these environments it was observed that the PCA has similar focusing properties as the ones described for the UWA channel considered in this section. For conciseness, only the environment described here will be examined because it is the most realistic of the cases considered. The other UWA channels that were considered include channels with different sound speed structures and different range-independent as well as range-dependent bathymetric features.

Roux and Fink (2000) performed similar analysis of the influence of combined array aperture and element spacing parameters on the extent of the focus in depth. Their work employed a ray-based model in a Pekeris waveguide. While some of these results are consistent with their findings, this analysis separates the influence of array aperture and inter-element spacing. A full-wave model is also employed here in an environment with a typical shallow water refractive profile. In addition, the vertical, horizontal, and temporal focusing are examined simultaneously as array parameters are modified.

A. Environmental characterization

The UWA environment used throughout this paper to study the usefulness of TRA in underwater communications is presented in Fig. 5. This UWA channel is range indepen-

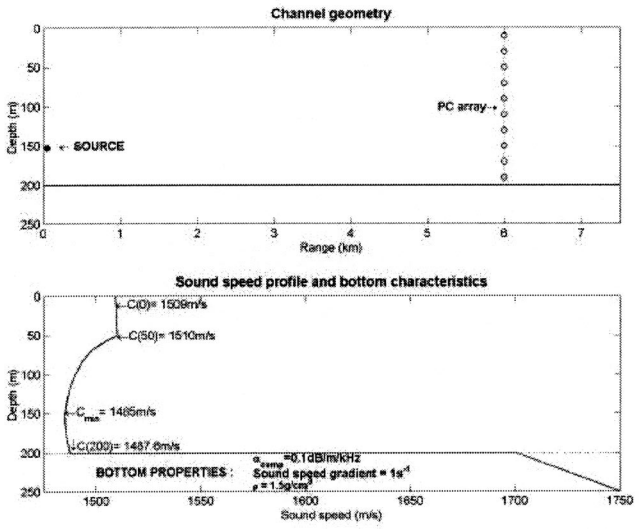

FIG. 5. UWA channel profile.

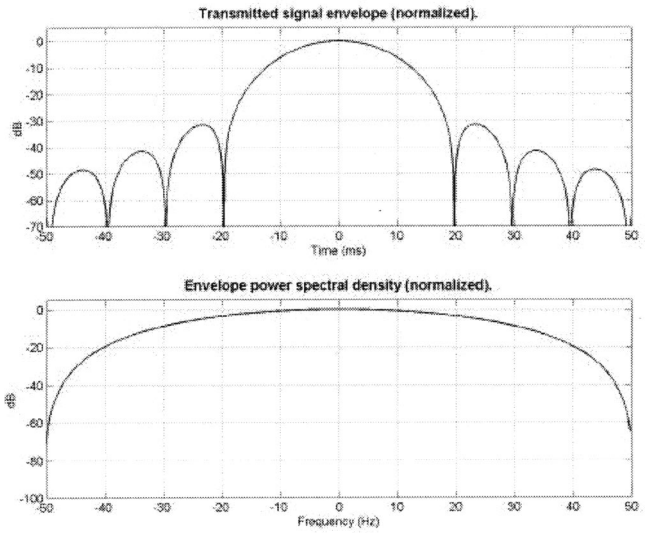

FIG. 6. Transmitted signal envelope.

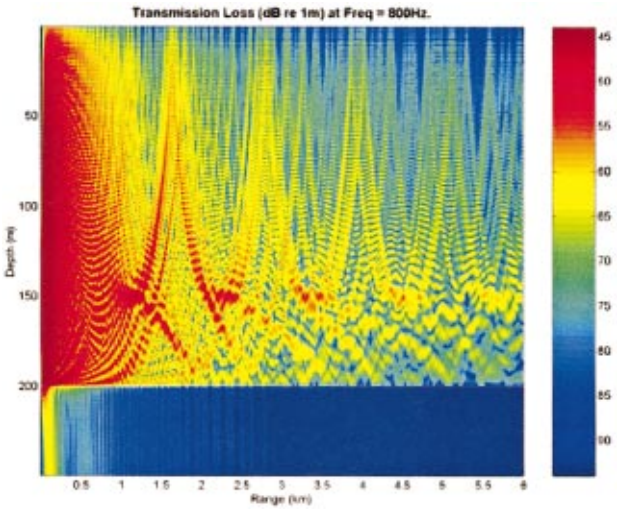

FIG. 7. Ocean response at 800 Hz.

dent in the sound speed profile, bottom bathymetry, and bottom acoustic properties. As depicted in Fig. 5, the source is located at a range of 0 m and a depth of 150 m, and the vertical PC array is located 6 km from the source. Throughout this section several array configurations will be used. In some cases the PC array may have different element spacing, in other cases it has different lengths and in some cases it can span the entire water column. In each instance, the issue to be considered is the impact on communications.

Figure 5 also shows the sound speed profile and the bottom characteristics. This environment has an upward refracting sound speed profile from a depth of 0 to 50 m. From 50 m to the bottom at 200 m, the UWA channel exhibits a sound speed profile similar to a typical shallow ocean sound speed structure with the sound axis located at 150 m in depth. The bottom has compressional attenuation of 0.1 dB/m/kHz, a sound speed gradient of 1 s^{-1}, and a density of 1.5 g/cm^3.

B. Transmitted signal envelope

In most of the TRA numerical simulations presented in this paper, the transmitted pulse has a carrier frequency of 800 Hz. The exceptions are in Sec. III D where carrier frequencies of 400 and 1200 Hz are also considered. In each case, the transmitted pulse has a bandwidth of 100 Hz with a −3-dB effective bandwidth of 36.6 Hz. The MMPE computational bandwidth over which the solutions of the PE field functions are computed includes the full 100 Hz. The envelope characterization of the transmitted pulse is given in Fig. 6. The spectrum of the transmitted pulse envelope is given by the coefficients of a Hanning window (Proakis and Manolakis, 1996). Therefore, the lower panel in Fig. 6 represents a Hanning window (in dB units) that spans 100 Hz in frequency. The time domain representation of the corresponding signal at a carrier frequency of 800 Hz can be found in the upper panel of Fig. 3. For this signal, the −3-dB pulse width is 14.1 ms.

C. Time-reversal acoustics in a range-independent environment

For the environment described in Sec. III A, Fig. 7 represents the magnitude of the ocean response for a time-harmonic acoustic source at a frequency of 800 Hz in a vertical plane defined by the source and the array elements. The ocean frequency response at 800 Hz is represented in terms of transmission loss (dB *re* 1 m). The complex multipath nature of the propagation is evident.

Considering the ocean as a spatial filter, Fig. 7 represents the forward propagation transfer function at the frequency of 800 Hz. The term ''forward propagation'' is used to denote the propagation from the acoustic source. If the source located at a depth of 150 m transmits a pulse at the carrier frequency of 800 Hz with a bandwidth of 100 Hz (−3-dB effective bandwidth of 36.6 Hz), the time arrival structure at the vertical array may be evaluated by Fourier synthesis of single frequency (CW) solutions over the bandwidth of interest. The time and frequency domain characterization of the transmitted pulse was previously described in Fig. 6.

Figure 8 represents the time arrival structure of the received signal envelope at the PCA for the 800-Hz signal with 100-Hz bandwidth. For a given array element, the envelope of the received signal is given by the corresponding horizontal line at the array element depth. The effects of multipath propagation are clearly observed in Fig. 8 where any array element detects several arrivals. From Fig. 8 one can see that the multipath structure is similar between closely spaced array elements. The diversity between array elements can be exhibited by computing the envelope cross-correlation of the time arrival structure represented in Fig. 8. The envelope cross-correlation shown in Fig. 9 was computed with respect to the envelope received by the array element at a depth of 150 m. With respect to this array element one can observe that the other array elements become more decorrelated as the depth difference between array elements increases. In general, as the distance between array elements increases, the multipath structure becomes more decorrelated. This spatial decorrelation between array elements is due to the presence

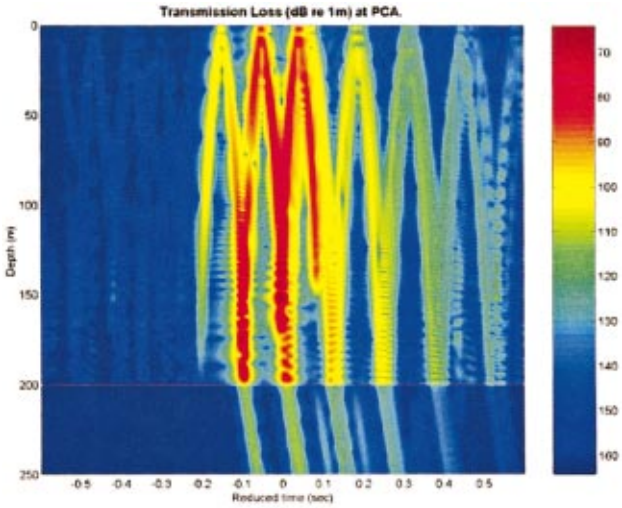

FIG. 8. Time arrival structure at the PCA.

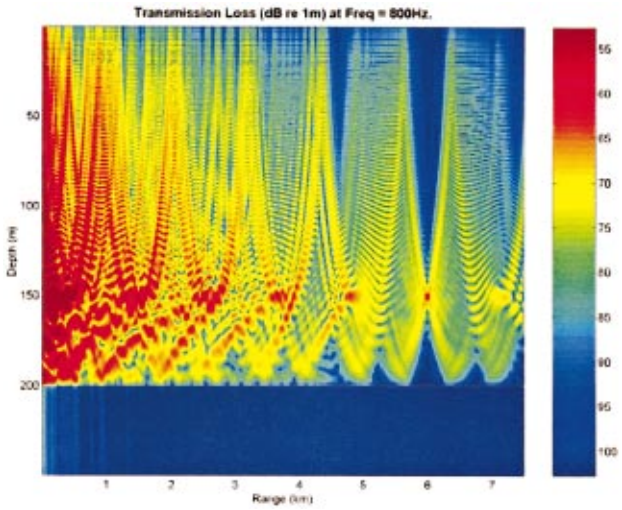

FIG. 10. Backward propagation ocean response at 800 Hz.

of multipaths and is used in communication systems that explore the spatial diversity in the water column.

At the PCA, the received signals are time reversed and transmitted back to the source. Figure 10 represents the ocean frequency response to the time-reversed acoustic field transmitted by the PCA evaluated at 800 Hz. The use of term ''backward propagation'' is meant to describe propagation of the time-reversed signals from the PCA through the reciprocal environment. From this perspective, Fig. 10 represents the backward propagation ocean frequency response at 800 Hz.

In Fig. 10, the propagation is from the left to the right, i.e., the PCA is located at range 0 km and spans the entire water column. In this geometry the original source is located at a range of 6 km and at a depth of 150 m. As expected, the phase conjugation of the 800-Hz frequency component and its consequent propagation through the channel produces a strong spatial focus at the source location.

As described in the previous section, when utilizing TRA the ocean itself behaves much like a spatial matched filter. Due to spatial reciprocity, the only location in space where this spatial filter is matched to the forward propagation function is at the source location. Therefore the output of this spatial filter is maximized at the source location, creating a strong focusing effect because the source location is the spatial location where the backward propagation transfer function matches the forward propagation transfer function. In other words, at the source location all multipath contributions will arrive in phase and add constructively, creating the focusing effect. Using these same arguments, all the other frequency components of the transmitted pulse will focus at the source location.

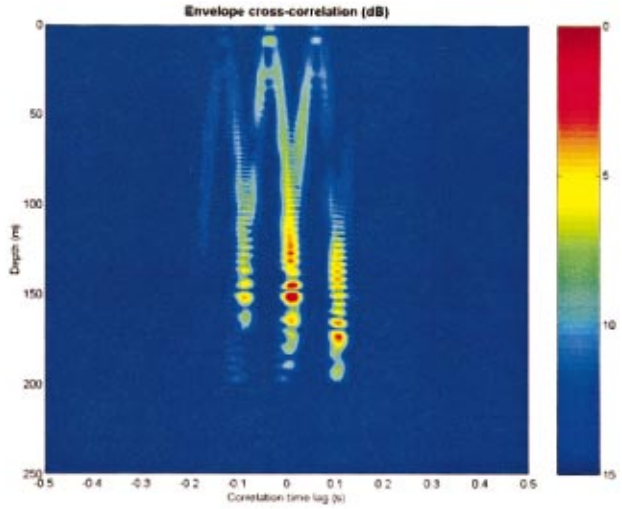

FIG. 9. Envelope cross-correlation across the array elements.

Figure 11 represents the time arrival structure of the backward propagated pulse ($f_c = 800$ Hz, $BW = 100$ Hz) at the source range and the temporal, vertical, and horizontal PCA focusing properties. The data displayed corresponds to the recorded signals of a vertical array of elements that spans the entire water column at the source range. This temporal focusing is also a consequence of the matched filter behavior of the ocean where all frequency components will arrive at the same time at the same location. Previous analysis of such focal regions in a different environment has been performed by Kuperman *et al.* (1998) and Song *et al.* (1998).

In this numerical simulation, the PCA spans the entire water column with an element spacing of $d = 0.244m$ and $\lambda/d = 7.67$, approaching the ideal case of a continuous line of sources. As a consequence, the temporal sidelobes represent the limiting situation that can be achieved in practice. As will be confirmed in this section, decreasing the number of array elements increases the temporal sidelobes.

Also note in Fig. 11 the vertical (along the depth) sidelobes of the focus. As mentioned in Sec. II, the vertical focusing is a consequence of the closure property of the propagating modes. Thus, these sidelobes appear in part because there are higher order modes that decay rapidly in range and do not propagate in the channel. In addition, some propagating modes are attenuated differently by the environment. Thus the focusing extent is dependent on the number of modes allowed in the channel.

Also displayed in Fig. 11 is the horizontal focusing at the source depth. This plot is very representative because it

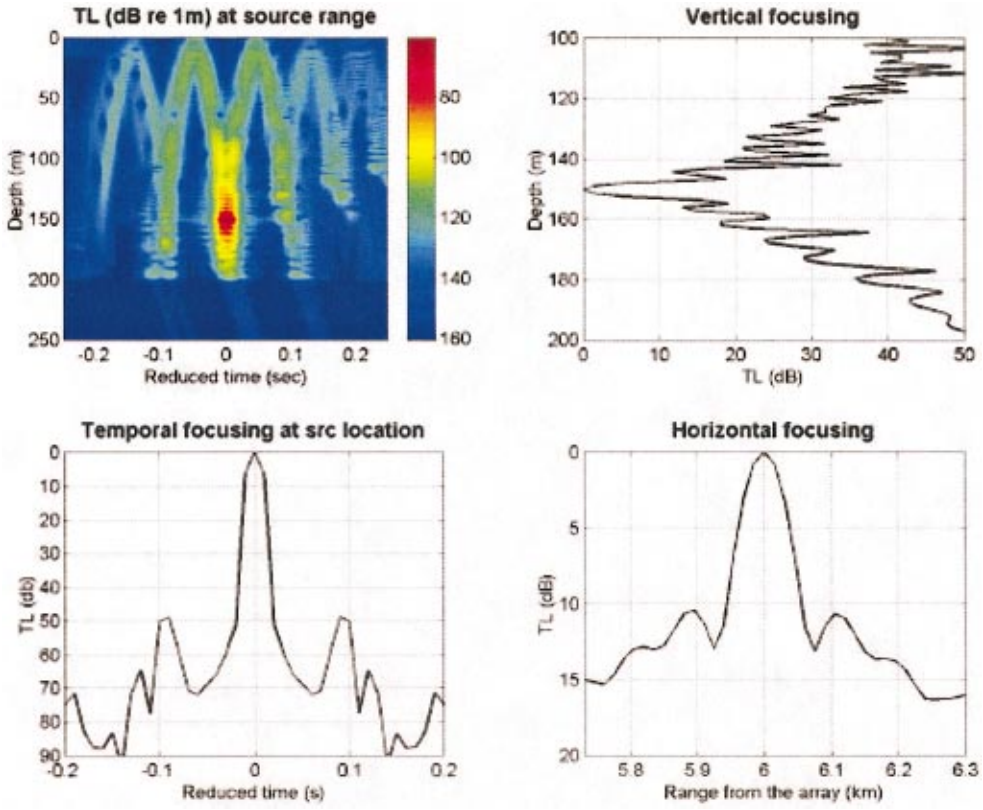

FIG. 11. Time arrival structure focus range. Temporal, vertical, and horizontal PCA focusing properties.

gives the maximum amplitude of the received signal envelope for a given location in range. The main lobe is located at 6 km corresponding to the source range and the −3-dB main lobe width is about 60 m, much larger than the corresponding value along the depth which is 3.3 m.

D. Focusing at different frequencies

In this analysis, three signals with carrier frequencies of 400, 800, and 1200 Hz were used. All these signals have the same bandwidth of 100 Hz that corresponds to a −3-dB effective bandwidth of 36.6 Hz, the same envelope spectral shape as described by Fig. 6, and the PC array spans the entire water column. The temporal, vertical, and horizontal focusing properties for each signal are displayed in Fig. 12.

As can be seen in Fig. 12, the temporal duration of the main arrival is identical for any of these test signals. This is a significant result because it means that use of the same bandwidth at different carrier frequencies achieves the same temporal pulse resolution and consequently the same symbol rates. It appears that the channel frequency response does not change significantly over the bandwidth of each signal and therefore the same temporal resolution exists at these different carrier frequencies. The temporal sidelobes are below 40 dB and decrease with increasing frequency. This is presumably due to the increase in the number of propagating modes at higher frequencies. In addition, the focus dimensions (or ''footprint'') are found to decrease with increasing frequency. This is due to a combination of the increase in the number of propagating modes and the decrease in acoustic wavelength.

E. Effect of interelement spacing

We now evaluate the influence on the focus due to PC arrays with different element spacing. Kuperman *et al.* (1998) previously examined the influence of reduced aperture and interelement spacing (to be considered next) on the focal region for their experimental results in the Mediterranean. A numerical analysis is presented here for our geometry/environment to provide insight into what PCA geometries may be acceptable for an underwater acoustics system.

In this case, the transmitted signal has a carrier frequency of 800 Hz and a bandwidth of 100 Hz. The geometry of the different PC arrays used in this study is given in Fig. 13 where each array is identified by a number from 1 to 6. Associated with each PCA are three numbers giving the number of elements, the distance between consecutive elements in meters, and the distance between consecutive elements in terms of carrier wavelengths. Note that PCA no. 1 has the smallest element spacing and that the distance between array elements doubles between consecutive arrays.

Starting from PCA no. 1 to no. 6, as the element spacing increases, the array cannot provide enough spatial sampling of higher-order propagating modes. Thus, the focusing degrades as a result of the lack of resolution of higher-order modes in the field. This change in focus is the result of removing array elements that are more correlated, i.e., as the array spacing increases it decreases the correlation between array elements.

From Fig. 13, one may conclude that the spatial dimensions of the focus do not change significantly for these PCA

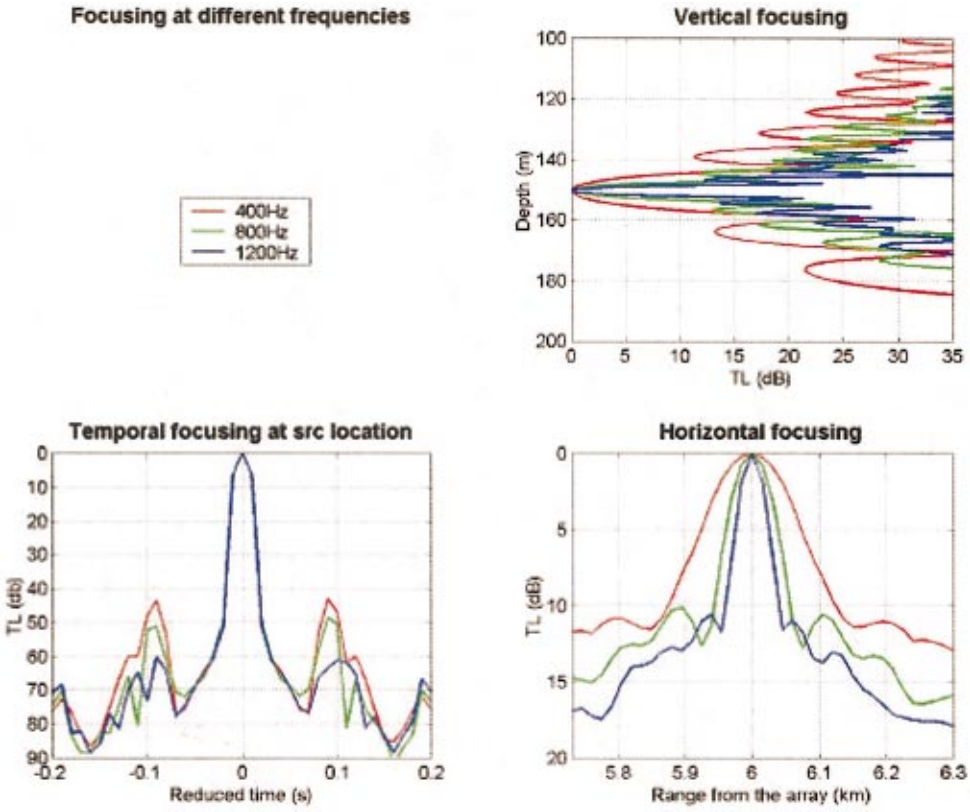

FIG. 12. Focusing at different frequencies.

configurations. Comparing these results to Fig. 11 where the PCA spans the entire water column one should expect an increase in temporal sidelobes because the PC arrays in Fig. 13 only span half of the water column, collecting less information about the channel conditions. Rather remarkably, in the worst case situation (PCA no. 6 with only nine elements), the temporal sidelobes are 25 dB below the main lobe. As the number of array elements increases, the temporal sidelobes improve 10 dB and become more defined.

The results in Fig. 13 seem to indicate that even with a

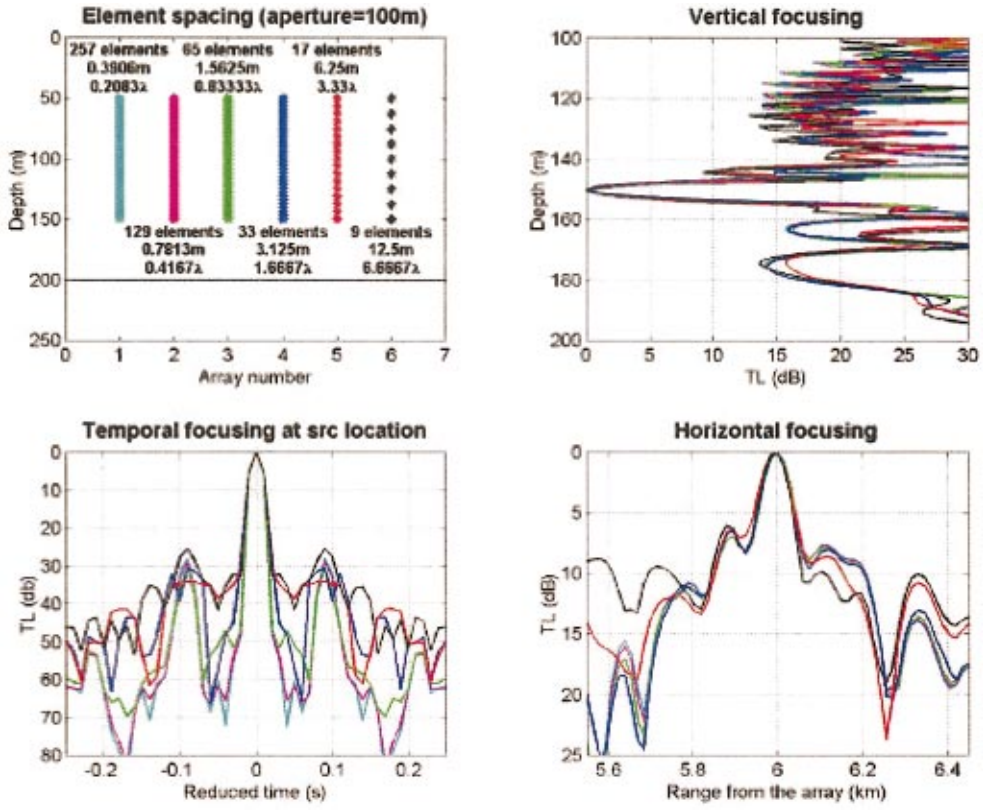

FIG. 13. Focusing properties using PC arrays with different element spacing.

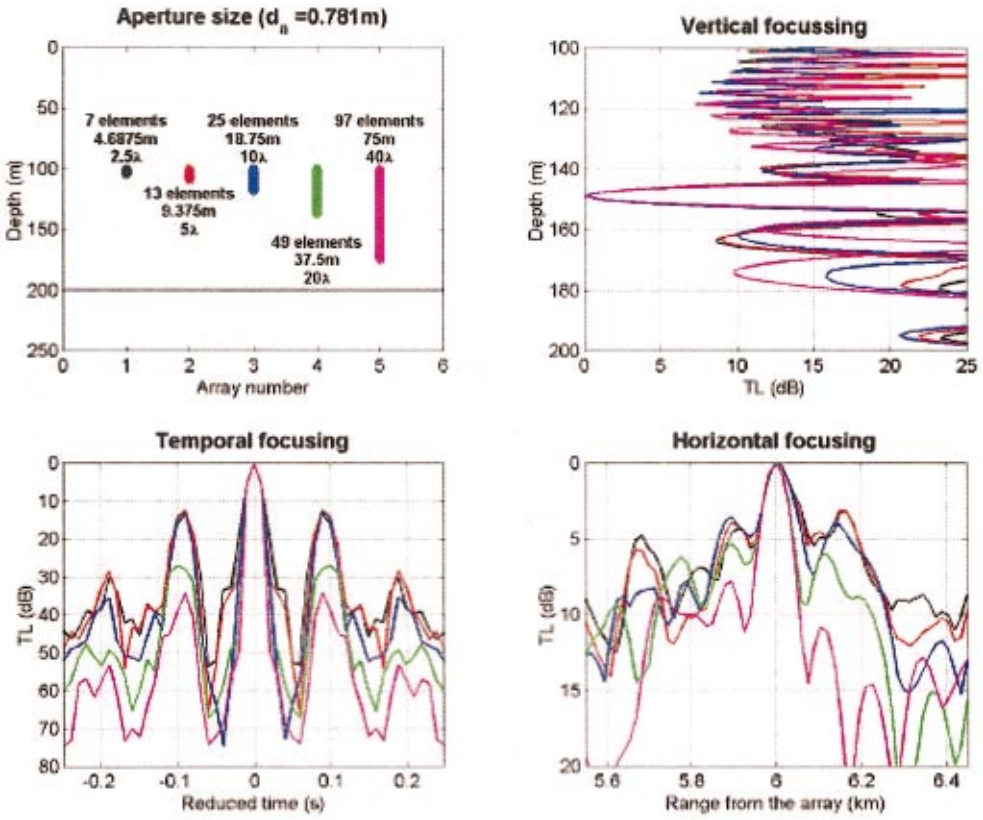

FIG. 14. Focusing properties using PC arrays with different aperture size.

small number of array elements, a good focusing quality, both temporally and spatially, can be achieved provided that the PCA has enough spatial sampling of the propagating modes in the water column. This also suggests that, in this environment, only a small number of the lowest propagating modes dominate the structure of the field and, therefore, the focus. This is important when considering the design of a communications array which employs TRA since the cost increases with the number of elements. Fortunately, it appears that a reduced number of array elements can maintain the temporal resolution, which relates to the data transfer rate at one focal point, and may still be able to take advantage of the spatial diversity of the field at the focal range, allowing multiple focal points in depth to further increase the data rate.

F. Effect of aperture size

In this study, the element spacing is kept constant in order to evaluate the effect that different PCA aperture sizes have on the focus quality. The geometry and spatial location in the water column of the different PC arrays is depicted in Fig. 14. In this figure, each array is designated by a number from 1 to 5. The numbers associated to each array give the number of array elements and the array length in meters and in carrier wavelengths. As the PCA aperture size increases, it can provide a better sampling of the low-order propagating modes. Starting with array no. 1 and going to array no. 5, the changes in focus are due to better spatial sampling of the low-order propagating modes. Thus, one should expect better focusing properties as the aperture size increases because the PCA has more spatial diversity and provides a better sampling of the channel conditions.

Because these PCA arrays cannot properly sample low-order propagating modes, the sidelobes increase in the depth and range coordinates. In Fig. 14, the first three arrays with apertures of $2.5\lambda_c$, $5\lambda_c$, and $10\lambda_c$, respectively, have temporal sidelobes about 12 dB below the main lobe. When the aperture size increases to $20\lambda_c$ the temporal sidelobes decrease to 27 dB below the main lobe. This distinctive behavior of array no. 4 compared to the other three is due to better sampling of the lowest-order propagating modes and therefore better temporal properties.

Presumably, the placement of these arrays in depth will also affect the focus quality. The best quality focus would be expected when the array is placed at a depth which optimally samples the dominant propagating modes. The conclusion that can be drawn is that in a given environment one should evaluate the most important propagating modes and use an array aperture that provides enough sampling of these modes.

IV. APPLICATION OF TIME-REVERSAL ACOUSTICS TO SHALLOW WATER COMMUNICATION SYSTEMS

In this section, we introduce a novel signaling scheme which takes advantage of the focusing properties of TRA system in a point-to-point acoustic link. The communication system described here uses a reduced-complexity noncoherent detector at the expense of increased complexity in the transmitter (PCA). The examples illustrated correspond to a nominal signaling rate of 30.5 symbols/second where 4 bits of information are encoded in each symbol. The channel used for numerical simulations is the one described in Sec.III A

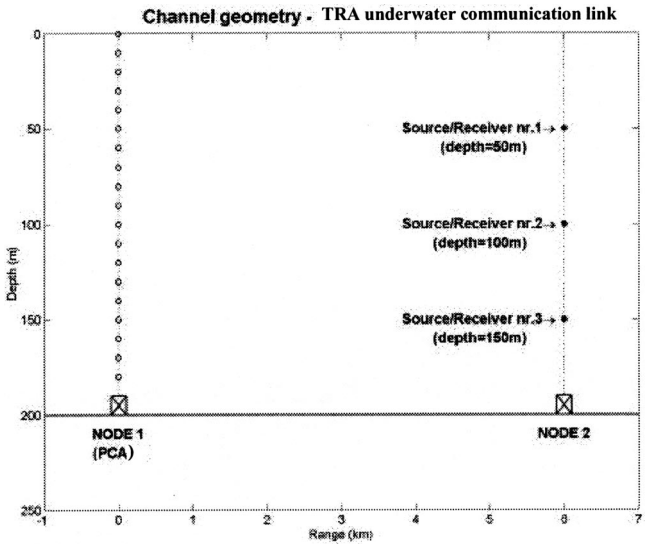

FIG. 15. PCA and channel geometry in a point to point communication link.

A. Using phase-conjugated arrays in underwater acoustic communications

Figure 15 can be used to describe the simplest case of point-to-point communications between two stationary communication nodes. Node 1 of Fig. 15 has a PC array that spans the entire water column, and a single source/receiver element of node 2 is used at a depth of 150 m. (The other source/receiver elements of node 2 will be utilized later.)

The first step towards the focusing of the node 1 PCA requires a probe pulse transmission from the node 2 acoustic source (nr. 3 in Fig. 15). As this probe pulse propagates, it will incorporate channel distortions including multipath. In the next step, the received acoustic signals at each node 1 element are digitized and stored in digital memories. For node 1 transmission (or backpropagation), the recorded signals will be time-reversed and transmitted by each node 1 element. The time-reversal transformation at the PCA is a simple task to perform, requiring the digital memories to be read in a last-in-first-out (LIFO) manner. At the PCA transmission, each element is excited by the output of the corresponding memory where the received signals were recorded. At this point one can consider that the PCA is ''focused'' at the nr. 3 source/receiver location of node 2 because it has recorded the necessary environmental information to generate a spatial focus at the node 2 source/receiver location.

The PCA's focusing procedure is a critical aspect in a TRA communication link. In a real situation, one must take into account the temporal variability of channel conditions. Focusing will degrade with time and will require periodic PCA refocusing. Additionally, the nodes may have some motion in general and the PC array may need to update the environmental information every time the receiver moves out of focus. In such a situation, the range shifting property of PC arrays discussed by Song *et al.* (1998) may be a very useful feature in a UWA communication system. If the receiver is moving slowly, the PCA is able to keep the focus at the receiver location, decreasing the rate at which the UWA communication system updates the environmental information (probing).

As a final remark, the electronic circuitry associated with each PCA element includes a receiver amplifier, an A/D converter, digital filters, memory, a D/A converter and a transmitter amplifier. Until this point no reference was made of the presence of digital filters at each PCA array element. A discussion of filter options is presented in the next section.

B. Signaling scheme

In this signaling scheme, each symbol represents a 4-bit word giving a total of 16 different words in the code. Since this communication system is based on noncoherent detection, the value of each bit within a symbol is given by the detection or lack of detection of the corresponding frequency component. There are 15 different symbols in the code having at least one spectral component. The ''all-zeros'' word corresponds to the case where no carrier frequencies are detected. This signaling scheme corresponds to a four channel ''on-off'' keying modulation scheme. Thus, a simple receiver can be built based on a four-element filter bank followed by an envelope detector. The detection of a given frequency component is achieved when the corresponding envelope detector output is higher than a given threshold.

In this scheme, four frequency components are defined centered at 750, 800, 850, and 900 Hz. Each one of these frequency components spans 100 Hz in frequency and has a -3-dB bandwidth of 36.6 Hz. The least significant bit corresponds to the frequency component centered at 900 Hz and the most significant bit corresponds to the component at 750 Hz.

To simplify the transmissions of the probe signals, assume that each PCA element has a bank of four digital filters centered at 750, 800, 850, and 900 Hz. Each source at node 2 must then transmit a single probe pulse covering the entire bandwidth, 700 to 950 Hz. An alternative approach would be for each source at node 2 to transmit each 100-Hz bandwidth probe pulse separately. If this last approach is chosen, there is no requirement for a digital filter bank in each PCA element but each node must make sure that the probe pulse transmissions will not overlap in time at the PCA.

The choice of which approach to use may be dictated by the temporal variability of the channel conditions that will degrade focusing and will require periodic update of the channel conditions. The filter bank approach has the advantage that it requires only one probe pulse transmission from each node 2 source in Fig. 15. Thus the communication system spends less time in array focusing and higher data throughput can be attained at the expense of a more complex PCA. However, the transmission of each individual probe pulse has the advantage of allowing the use of matched filters at reception. This may provide additional SNR gain and be more robust to signal fading.

C. The phase-conjugated array

In this section, it is assumed that the PCA is able to learn the environmental information in the bandwidth of interest. The PCA is not in a shadow zone and each source transmits

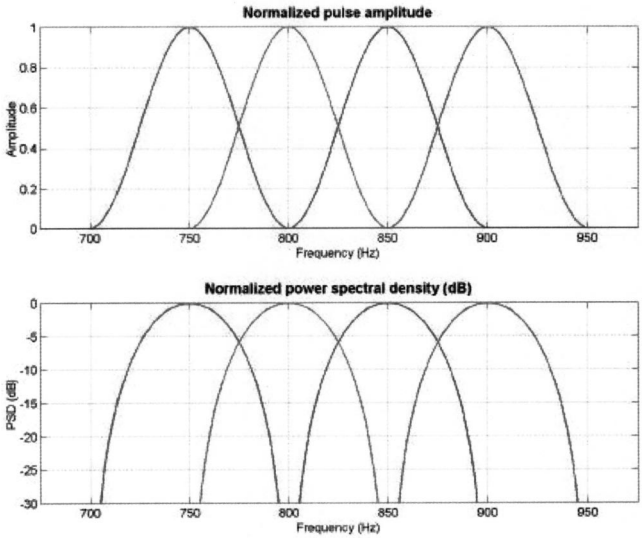

FIG. 16. PCA element filter bank frequency response.

a probe pulse with bandwidth wide enough to accommodate the bandwidth used to transmit all individual frequency components of the signaling scheme.

The signaling scheme described in the previous section requires a four-element filter bank for each PCA element. This four-element filter bank frequency response is given in Fig. 16. All the filters have the same spectral shape but different center frequency, each filter frequency response spanning over 100 Hz, giving a −3-dB bandwidth of 36.6 Hz. The frequency response of each filter is specified by the coefficients of a Hanning window. In Fig. 16, the center frequency of each filter corresponds to the center frequency of one of the frequency components used in the signaling scheme.

After PCA reception and filtering, each PCA element will have recorded four different signals with different center frequencies. Each one of these signals will have the transfer function of the channel imprinted on it. As seen in the previous section, if all PCA elements transmit only the signal component centered at 800 Hz, a pulse with 800 Hz carrier frequency and a −3-dB bandwidth of 36.6 Hz will be received at the node 2 focus location.

D. Point to point message transmission

This section presents a numerical simulation where a message is sent from node 1 to node 2 of Fig. 15. At each PCA element, the transmitted signal corresponding to a given symbol can be obtained by time-domain superposition (i.e., simultaneous transmission) of its different frequency components. Similarly, the signal corresponding to a sequence of symbols can be obtained by superposition of the signals corresponding to the different symbols, properly delayed in the time domain. This time-domain delay corresponds to the signaling period and should be greater than the temporal duration of each symbol at the receiver location to avoid intersymbol interference. In this case, each single frequency component will have at the receiver a −3-dB temporal duration of 14.1 ms and a conservative value of 32.8 ms was chosen for the signaling period.

Figure 17 presents the spectrograms of the signal corresponding to a message composed by the sequence of words from $(0001)_b$ to $(1111)_b$ that is intended to be transmitted from node 1 to the node 2 receiver. The upper panel represents the ideal signal that node 1 wants to focus at the node 2 receiver. The other panels in Fig. 17 present the results from a numerical simulation where node 1 spans the entire water column and transmits the appropriate signals to focus the message at the node 2 receiver. All the signals in Fig. 17 are collected at a depth of 150 m. The middle-left panel represents the signal transmitted from the PCA element located at 150-m depth while the other three correspond to the signal spectrogram at various ranges. Only the lower right panel in Fig. 17 corresponds to the signal spectrogram at the focus location.

In Fig. 17 one can clearly observe that as the pulse backward propagates in the channel the multipath structure becomes less significant as the range approaches the focusing range. It can also be seen that when the pulse approaches the focusing range it increases the power spectral density of its spectral components. This increase in the power spectral density is a consequence of the vertical, horizontal, and temporal PCA focusing properties as the sequence of symbols approaches the focus location.

E. Phase-conjugated array vertical diversity in underwater communications

Presented in this section is an extension of the TRA technique which takes advantage of vertical diversity of the focus. The setup for this TRA experiment is depicted in Fig. 15 with the difference that node 2 has now three source/receiver elements. The extension of the TRA technique presented here exploits node 1 PCA vertical diversity to focus the backward propagated acoustic field at the different node 2 receiver locations. As a result, higher data throughputs can be achieved in the data link from node 1 to node 2.

In this case the PCA focusing process requires probe pulse transmissions from each source/receiver element of node 2. The transmission of probe pulses from node 2 has the constraint that it must allow enough time between consecutive transmissions so each pulse will arrive at node 1 at different time slots and the pulses do not interfere. In this example, node 1 will require a data bank with three times the storage capacity of the one used in node 2 because it has to store the signals received from three probe pulses. The TRA acoustic link from node 1 to node 2 can accommodate three times the data throughput of the case presented in the previous sections. In this case, node 2 has three receivers and node 1 is able to send three different symbols (one for each node 2 receiver) during each symbol period.

At transmission, the PCA will assemble the message intended for each receiver by the superposition of its frequency components stored in its data bank. The signal transmitted by each PCA element will be composed of the superposition of the signals for the different node 2 receivers. Figure 18 represents the desired message signal spectrogram that the PCA wants to focus at each node 2 receiver. Note that these signals do not correspond to the actual signals sent by the node 1 elements.

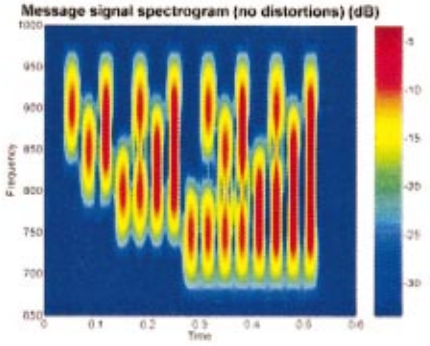

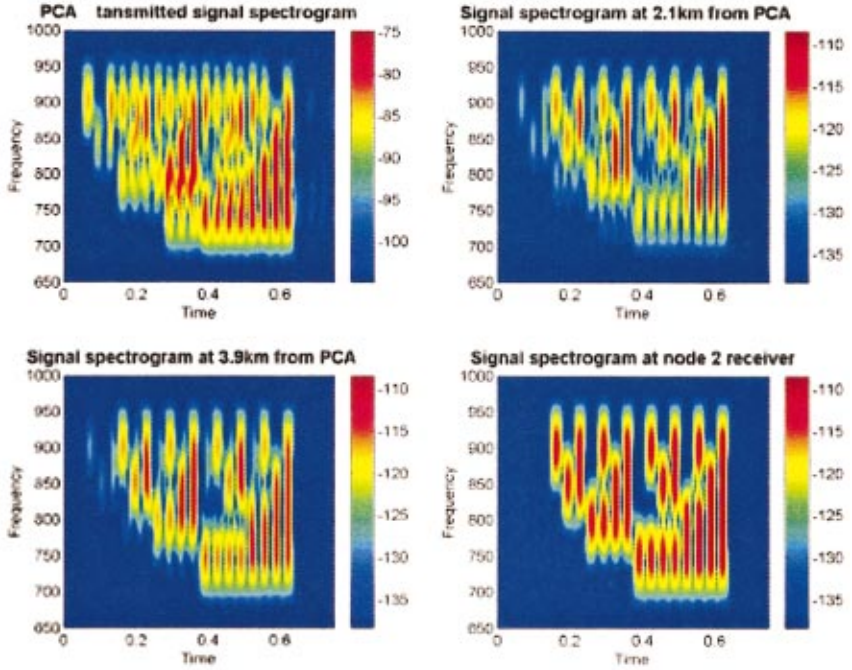

FIG. 17. The central upper panel displays the desired message if no distortions are present in the channel. Other panels display message signal spectrograms at a depth of 150 m dp: (middle left) evaluated at the PCA (transmitted); (middle right and lower left) at two intermediate ranges; and (lower right) at the focus.

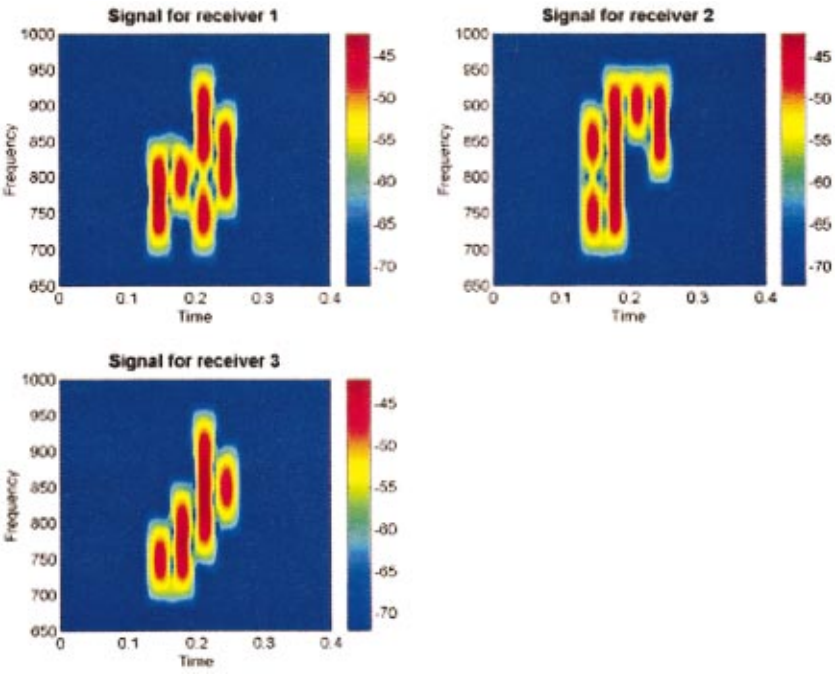

FIG. 18. Desired message signals for node 2 receivers.

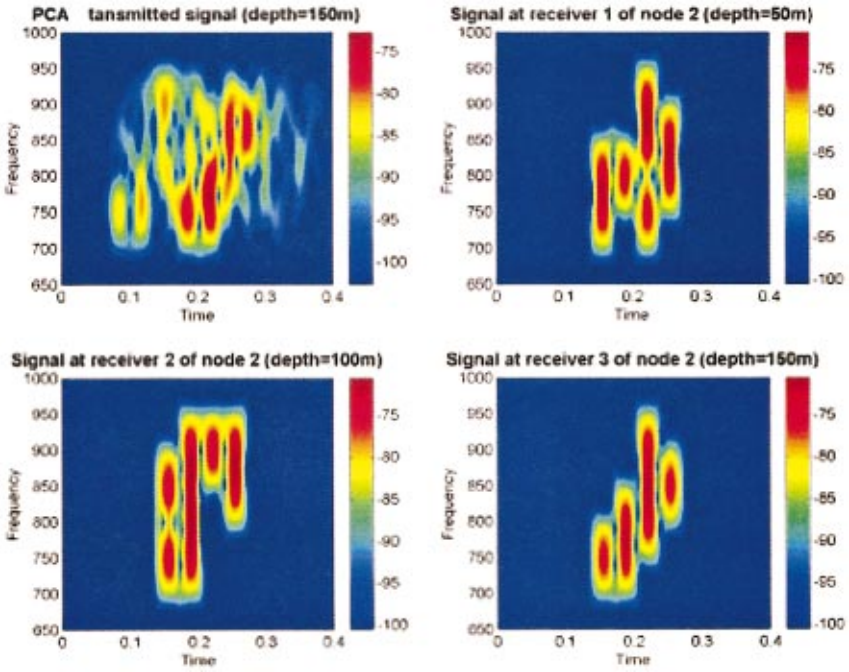

FIG. 19. Transmitted signal by PCA and received signals at node 2 receivers.

Figure 19 presents numerical simulation results of the PCA transmitted signal propagation in which Fig. 18 represents the message that the PCA wants to focus at each receiver location. In this simulation, the PCA spans the entire water column and the upper-left panel of Fig. 19 represents the actual signal sent by the element located at a depth of 150 m. We can observe multipath structure and strong interference between the different transmitted messages. The remaining panels in Fig. 19 represent the signal received by each one of the node 2 receivers. Due to the vertical focusing properties of the PCA, these results show very little message intersymbol interference at each receiver and the desired message can be easily decoded.

With respect to this same numerical simulation, Fig. 20 represents the signal spectrogram at different ranges between node 1 and node 2 collected at a depth of 150 m. The results in this figure show that it will be extremely difficult to decode the original messages at these locations because the different message signals are overlapping both in time and in frequency. These results also show that this TRA vertical diversity technique may have applications to UWA secure communication links. Channel distortions and signal overlap both in time and frequency of the different messages seems to be a very good way to encode digital communication signals with the advantages of a higher data throughput. Such encoding also occurs for the single focus approach described previously but does not exhibit the same level of encryption.

Additional simulations were also performed which took

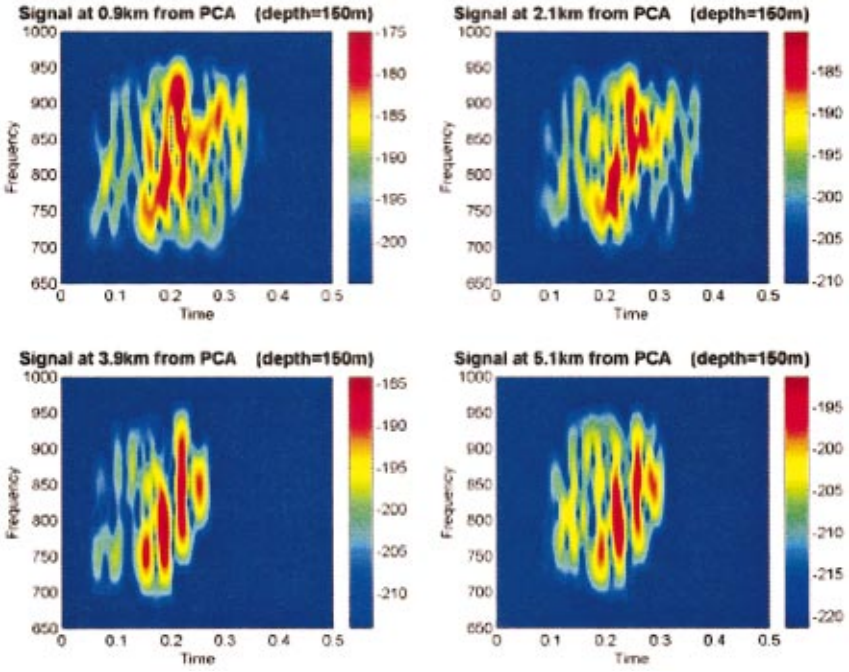

FIG. 20. Received signal spectrogram at depth of 150 m and different ranges from PCA.

advantage of the horizontal spatial diversity of the time-reversed field. Specifically, a network of nodes, separated from the PCA by different ranges, was employed. Similar results were obtained whereby each individual node (some containing multiple receiving elements in depth) received unique focused signals at the particular location for that node. This suggests the potential for an extended area network. However, the signaling schemes for such a configuration would be considerably more complex at the PCA.

V. CONCLUSIONS

In this paper, we numerically explored the influences of a phase-conjugation array design on its focusing properties. Particular attention was given to PCA applications in UWA communication systems. This analysis provides a starting point for a PC array design, and gives support to the planning of further TRA UWA communication experiments both in the laboratory and in an oceanic environment. In the early stages of a TRA UWA communication system design, TRA numerical modeling is very important because it gives insight to the propagation issues that are involved without the need to go out to the ocean and perform very expensive experiments. However, although numerical modeling is an excellent analysis tool, it does not provide complete information about time-variability of the channel conditions.

The numerical analysis of the PCA focusing properties showed that the focus footprint decreases in dimension as the carrier frequency increases. Furthermore, the horizontal dimension is larger than the vertical dimension of the footprint. Therefore vertical motion of the receiver is much more critical than horizontal motion because the receiver can easily move out-of-focus.

Using the same bandwidth and changing carrier frequency, results showed that temporal focusing does not change significantly. However, in a more general situation where a larger pulse bandwidth is used, additional results suggested that for carrier frequencies much higher than 1 kHz, some degradation may occur in the pulse temporal resolution at the focus location since the two-way channel frequency response may change considerably over the bandwidth.

When using PC arrays with different element spacing or with different aperture size, the PCA footprint did not appear to change its dimensions. Keeping constant the aperture size and changing the PCA element spacing, the temporal sidelobes remained approximately at the same level. Keeping constant the PCA element spacing and changing the aperture size, the vertical and horizontal footprint size also did not appear to change significantly. A small improvement in horizontal sidelobes was observed when the aperture length was increased. A dramatic improvement in temporal sidelobes was observed when the aperture size increased to $20\lambda_c$ because the PCA was able to provide better spatial sampling of the lowest propagating modes. In other words, there was more spatial diversity in the PC array.

What may be concluded from this analysis is that aperture size plays a more significant role than the number of array elements in a PC array design, especially for communication applications where temporal resolution of the focus is important. The number of PCA transducers is a critical factor in PC array design because it will drive up the cost. Each PCA transducer has its own electronic circuitry composed of receiver amplifiers, A/D and D/A converters, storage memory, and transmitter. In general, underwater devices rely on batteries to operate their electronic systems and have severe constraints on the amount of power that can be used. Thus, for cost effectiveness one should use a small number of array elements extended over a large aperture size.

For UWA communication systems using noncoherent detection, the use of PC arrays seems promising because there is no requirement of carrier phase tracking. The temporal focusing properties of the PCA overcomes the requirement of guard times between consecutive symbols to ensure that all the reverberation will vanish before each subsequent symbol is received avoiding intersymbol interference at the receiver. Thus some data rate improvement is made because the insertion of idle periods of time results in a reduction of the available data throughput. Array processing is no longer required because the PCA footprint is well defined at the receiver location.

The data throughput can be further improved by taking advantage of the PCA spatial diversity focusing properties. In the cases presented, the PCA was able to focus simultaneously different messages at different receiver locations. The message signal designated for a given receiver only focused at the intended receiver location. At the receiver the corresponding message signal was compressed in time and space and had higher magnitude than the other interfering message signals. As a consequence, each message signal could only be decoded at the desired receiver. Furthermore, this seems to be a good technique for secure UWA communications because the different message signals will be overlapping both in time and frequency at other locations, making it difficult to recover any of the transmitted messages.

Several of the features of this communications algorithm employing time-reversal acoustics have already been implemented experimentally at the Naval Postgraduate School in a controlled tank-scale environment. The results are consistent with those from numerical simulations. These findings will be reported in a companion article. The modeling work is now examining issues related to more realistic environments, while the experimental tank work pursues more sophisticated signaling schemes.

Due to the PC array spatial diversity focusing properties, PC arrays may have an important role in an acoustic local area network. Each array is able to simultaneously transmit different messages that will focus at the destination receiver node. Although the first protocols for acoustic local area networks have been proposed by Brandy and Catipovic (1994) and Talavage *et al.* (1994), the design of an acoustic local area network protocol that accommodates the learning step of the PCAs is still being developed.

In order to achieve high-speed data transmission, the use of TRA bandwidth-efficient phase-coherent communications requires further research. Due to temporal variability of channel conditions, the first step towards the feasibility of TRA phase-coherent communications is the evaluation of the phase-stability (phase fluctuations) at the focus. Once ac-

complished, the receiver structure can be determined and an adaptive equalizer can be designed to accommodate temporal variability of the channel conditions. Other approaches useful in communications should also be explored under these variable conditions, such as increased symbol information through amplitude modulation. Several such issues are currently be investigated at the Naval Postgraduate School.

ACKNOWLEDGMENT

This work was supported by ONR Code 321OA. The authors would like to acknowledge the help and guidance of Professor Monique Fargues, Naval Postgraduate School, for many useful discussions. We also wish to thank Dr. William Kuperman and Dr. William Hodgkiss, Marine Physical Laboratory, UCSD, and Dr. Milica Stojanovic for guiding us through some initial revisions.

Abrantes, A. A. M., Smith, K. B., and Larraza, A. (**1999**). ''Examination of time-reversal acoustics and applications to underwater communications,'' J. Acoust. Soc. Am. **105**, 1364 (joint conference of ASA, EAA, DAGA, 14–19 March, Berlin, Germany).

Baggeroer, A. (**1984**). ''Acoustic telemetry—An overview,'' IEEE J. Ocean. Eng. **9**, 229–235.

Brandy, D. P., and Catipovic, J. A. (**1994**). ''Adaptive multiuser detection for underwater acoustic channels,'' IEEE J. Ocean. Eng. **19**, 158–165.

Brienzo, R. K., and Hodgkiss, W. S. (**1993**). ''Broadband matched-field processing,'' J. Acoust. Soc. Am. **94**, 2821–2831.

Catipovic, J. (**1990**). ''Performance limitations in underwater acoustic telemetry,'' IEEE J. Ocean. Eng. **15**, 205–216.

Coates, R. F. W. (**1993**). ''Underwater acoustic communications,'' in *Proc. OCEANS'93*, Victoria, BC, pp. III.420–III.425.

Coates, R., Owens, R., and Tseng, M. (**1993**). ''Underwater acoustic communications: A second bibliography and review,'' in *Proc. Inst. Acoust.*

Galvin, R., and Coates, R. F. W. (**1994**). ''Analysis of the performance of an underwater acoustic communication system and comparison with a stochastic model,'' in *Proc. OCEANS'94*, Brest, France, pp. III.478–III.482.

Heinemann, M. G. (**2000**). ''Experimental Studies of Applications of Time-Reversal Acoustics to Non-coherent Underwater Communications,'' Naval Postgraduate School, Master's Thesis.

Henderson, G. B., Tweedy, A., Howe, G. S., Hinton, O., and Adams, A. E. (**1994**). ''Investigation of adaptive beamformer performance and experimental verification of applications in high data rate digital underwater communications,'' in *Proc. OCEANS'94*, Brest, France, pp. I.296–I.301.

Howe, G. S., Tarbit, P., Hinton, O., Sharif, B., and Adams, A. (**1994**). ''Subsea acoustic remote communications utilizing an adaptive receiving beamformer for multipath suppression,'' *Proc. OCEANS'94*, Brest, France, pp. I.313–I.316.

Jackson, D. R., and Dowling, D. R. (**1991**). ''Phase conjugation in underwater acoustics,'' J. Acoust. Soc. Am. **89**, 171–181.

Jackson, D. R., and Dowling, D. R. (**1992**). ''Narrow-band performance of phase-conjugate arrays in dynamic random media,'' J. Acoust. Soc. Am. **91**, 3257–3277.

Jensen, F. B., Kuperman, W. A., Porter, M. B., and Schmidt, H. (**1994**). *Computational Ocean Acoustics* (American Institute of Physics, Woodbury, NY).

Kuperman, W. A., Hodgkiss, W. S., Song, H. C., Akal, T., Ferla, C., and Jackson, D. R. (**1998**). ''Phase conjugation in the ocean: Experimental demonstration of an acoustic time-reversal mirror,'' J. Acoust. Soc. Am. **103**, 25–40.

Proakis, J. G., and Manolakis, D. G. (**1996**). *Digital Signal Processing: Principles, Algorithms, and Applications* (Prentice–Hall, Upper Saddle River, NJ).

Roux, P., and Fink, M. (**2000**). ''Time reversal in a waveguide: Study of the temporal and spatial focusing,'' J. Acoust. Soc. Am. **107**, 2418–2429.

Smith, K. B. (**2001**). ''Convergence, stability, and variability of shallow water acoustic predictions using a split-step Fourier parabolic equation model,'' J. Comput. Acoust. **9**, 243–285.

Smith, K. B., and Tappert, F. D. (**1994**). ''UMPE: The University of Miami Parabolic Equation Model, *Version 1.1*,'' MPL Technical Memorandum 432.

Song, H. C., Kuperman, W. A., and Hodgkiss, W. S. (**1998**). ''A time-reversal mirror with variable range focusing,'' J. Acoust. Soc. Am. **103**, 3234–3240.

Stojanovic, M. (**1996**). ''Recent advances in high-speed underwater acoustic communications,'' IEEE J. Ocean. Eng. **21**, 125–136.

Stojanovic, M., Catipovic, J. A., and Proakis, J. G. (**1993**). ''Adaptive multichannel combining and equalization for underwater acoustic communications,'' J. Acoust. Soc. Am. **94**, 1621–1631.

Stojanovic, M., Catipovic, J. A., and Proakis, J. G. (**1994**). ''Phase coherent digital communications for underwater acoustic channels,'' IEEE J. Ocean. Eng. **19**, 100–111.

Stojanovic, M., Catipovic, J. A., and Proakis, J. G. (**1995**). ''Reduced-complexity spatial and temporal processing of underwater acoustic communication signals,'' J. Acoust. Soc. Am. **98**, 961–972.

Talavage, J., Thiel, T., and Brandy, D. (**1994**). ''An efficient store-and-forward protocol for a shallow water acoustic local area network,'' *Proc. OCEANS'94*, Brest, France.

Tarbit, P. S. D., Howe, G., Hinton, O., Adams, A., and Sharif, B. (**1994**). ''Development of a real-time adaptive equalizer for a high-rate underwater acoustic data communication link,'' in *Proc. OCEANS'94*, Brest, France, pp. I.307–I.312.